



# The Near Field Properties of Colloidal Polystyrene Microspheres on Silicon

Sumei Huang<sup>1,\*</sup>, Zhengnan Wang<sup>1</sup>, Zhuo Sun<sup>1</sup>, Zengbo Wang<sup>2</sup>, and Boris Luk'yanchuk<sup>3</sup>

<sup>1</sup>Engineering Research Center for Nanophotonics and Advanced Instrument, Ministry of Education, Department of Physics, East China Normal University, North Zhongshan Rd. 3663, Shanghai 200062, P. R. China

<sup>2</sup>Laser Processing Research Centre, School of Mechanical, Aerospace and Civil Engineering, University of Manchester, Sackville Street, Manchester, M60 1QD, UK

<sup>3</sup>Data Storage Institute, DSI Building, 5 Engineering Drive 1, Singapore 117608, Republic of Singapore

We have investigated the optical resonance and near field inside and under absorptive polystyrene (PS) microspheres on Si wafers. Near field flat plane images of PS microspheres were numerically simulated. Nanostructures were prepared on Si substrates using the regular two dimensional (2D) arrays by a single pulsed laser irradiation (KrF,  $\lambda = 248$  nm). Periodical PS nanoparticle, PS nanoflowers and Si nanobumps were fabricated by different laser fluence. Mechanisms for PS particle size reduction and Si nanobump formation by laser irradiation were discussed on the base of the theoretical calculations. Good agreement between theoretical calculations and experimental results has been observed.

**Keywords:** Near Field Interaction, Mie Scattering, Laser Irradiation, Surface Nano-Patterning.

## 1. INTRODUCTION

Particles of different sizes, shapes and materials have been attracting much attention due to their unusual size, shape-dependent physical and chemical properties. Different techniques have been developed to generate crystals of spheres or to apply self-organized layers of colloidal spheres as masks for wet or dry patterning different shapes of particles, pillars, nanowires or nanocones.<sup>1-3</sup> Microstructures based on assembled or patterned particles have been used for many applications such as chemical sensors,<sup>4</sup> photonic crystals,<sup>5</sup> diffraction gratings,<sup>6</sup> light-emitting diodes,<sup>7,8</sup> and solar cells.<sup>9,10</sup> We have reported a method to use regular two-dimensional (2D) periodic lattices of micro- or nano-spheres for a single-step parallel surface patterning to generate hexagonal arrays of 2D holes, nanobumps and nanoparticles.<sup>11-15</sup> This nanofabrication method is based on the optical near-field effects under transparent or half transparent small sized spheres. The method is a high-speed parallel processing technique which permits single-step production of millions of holes/cones/nanoparticles with long-range order on the surface using a single or a few laser shots. In this nanofabrication, the calculation of the near field of micro or nano-spheres is a fundamental theoretical issue. However, most

of previous theoretical investigations based on Mie theory have not well explored the field characteristics inside the particle or the field interactions and coupling between the neighbouring particles.<sup>10-17</sup> Until recently, several theoretical attempts have been made to analyze the near field optics of a 2D periodic system on a substrate.<sup>18-22</sup> For example, the optical transmission through metal or silicon coated monolayers of microspheres and the field distribution in these monolayers were calculated by FDTD modeling.<sup>19-21</sup> Moreover, a commercial FIT software package (CST Microwave Studio 2006) was used for solving electromagnetic problems of hexagonal arrays of transparent particles with different sizes on metal films with Cartesian grids system (FDTD module).<sup>23</sup> The field interactions between the neighbouring particles were explored.

In this paper, we report the results of detailed investigation on the optical resonance and near field inside and under absorptive spherical polystyrene (PS) micro-particles on Si wafers by combining theoretical calculations with experimental studies. We present nanostructures fabricated on Si substrates using the regular 2D arrays by a single pulsed laser irradiation (KrF,  $\lambda = 248$  nm). Periodical PS nanoparticle, PS nanoflowers and Si nanobumps were fabricated by different laser fluence. The morphologies of the created nanostructures were characterized by an atomic force microscope (AFM) and a scanning electron microscope (SEM). Calculations of the field distribution of

\* Author to whom correspondence should be addressed.

absorptive sphere arrays on silicon were presented. Mechanisms for PS particle size reduction by laser irradiation were discussed.

## 2. EXPERIMENTAL DETAILS AND THEORETICAL CALCULATIONS

Hexagonally closed-packed PS colloidal monolayers were prepared on the surface by a self-organizing process. A polystyrene (PS) latex (Duke Science) was used. The diameter of PS particles is 1.0  $\mu\text{m}$ . Monodisperse PS microspheres were applied to a freshly purchased and undoped silicon (100) substrate after the suspension had been diluted with deionized water. The substrate was kept still until all of the water had been evaporated. As a result, a PS bead monolayer array with a large area was obtained on the Si surface. The PS sphere array was exposed to a single shot of a Lambda Physik LPX 100 KrF excimer laser with a wavelength  $\lambda = 248$  nm and pulse width  $\tau = 23$  ns. A 25 mm  $\times$  5 mm rectangular laser spot with uniform light intensity was used. The laser fluence is in the range from 20 to 300  $\text{mJ}/\text{cm}^2$ . The laser beam was incident normally on the sample with the particle array. Each sample was treated using a single laser pulse. The surfaces before and after laser treatment were observed with a high-resolution optical microscope. The features of the irradiated areas were characterized by an AFM and a scanning electron microscope (SEM).

CST Microwave Studio 2006 is a general purpose and full 3D microwave modeling platform that incorporates eigenmode, frequency and time-domain solvers for various applications.<sup>24</sup> The electromagnetic field distribution in a PS microsphere–bulk crystalline silicon substrate system was simulated by using this software. Upon choosing a suitably refined computational grid (the maximum grid length was chosen as wavelength/10 in the paper), the corresponding numerical solution gives an accurate representation of the dynamics of the electromagnetic field. The PS sphere with a diameter of  $2a$  is placed on the c–Si substrate. The origin of the coordinates is taken at the center of the sphere. The  $xy$  plane is set parallel to the surface of the substrate. The substrate is situated in the positive  $z$  region. There is a separation distance along the  $z$ -axis ( $g = 2$  nm) between the sphere and the c–Si surface. Let the plane-wave electromagnetic field of wave vector  $k$  be incident from the top of the sphere ( $z < 0$ ). The wave propagates along the  $z$  coordinate, the electric vector is along the  $y$  coordinate, and the magnetic vector along the  $-x$  coordinate. The top surface of the bulk Si is at  $z = a + g$ . The Transient Solver module of the CST software was used for this work. This module is a general purpose module of the 3D EM simulator.<sup>24</sup> We set the accuracy in the Solver Parameters menu at a setting of  $-80$  dB which means the transient solver stops at the moment when the remaining energy of the time signals

within the calculation domain decays to  $10^{-8}$  compared to the maximum energy. The computational domain is rectangular with dimensions  $-8a \leq x \leq 8a$ ,  $-8a \leq y \leq 8a$  and  $4a \leq z \leq 4a$ . A perfectly matched layer (PML) open boundary conditions were applied for all the boundaries of the computational domain (numerical reflection coefficient  $< 0.01\%$  with the typical four-layered PML).

In the next section, theoretical studies of the light interaction within the PS microsphere–c–Si system are presented. The optical constants of PS at 248 nm were fitted by the Drude dielectric function:

$$\varepsilon(\omega) = \varepsilon_{\infty} - \frac{\omega_p^2}{\omega(\omega + i\nu_c)} \quad (1)$$

where  $\omega_p$  is the plasma frequency,  $\nu_c$  the electron collision frequency and  $\varepsilon_{\infty}$  the infinite frequency permittivity. The optical constants of PS from Ref. [25] in the visible range were fitted by Eq. (1). The fitted values of  $\varepsilon_{\infty}$ ,  $\omega_p$  and  $\nu_c$  for PS are 2.543,  $9.063 \times 10^{16}$   $\text{rad} \cdot \text{s}^{-1}$ ,  $9.087 \times 10^{15}$   $\text{s}^{-1}$ , respectively. Furthermore, the optical constants of bulk crystalline silicon were fitted by Lorentz oscillator model:<sup>26</sup>

$$\varepsilon(E) = \varepsilon_1(\infty) + \sum_{j=1}^4 \frac{A_j}{E_j^2 - E^2 - i\Gamma_j E} \quad (2)$$

where  $\varepsilon_1(\infty)$  refers to the dielectric constant at very large photon energies,  $A_j$  is the amplitude of the  $j$ th oscillator with the unit of  $(\text{eV})^2$ ,  $\Gamma_j$  is the damping factor of the  $j$ th oscillator with the unit of eV, and  $E_j$  is the resonant energy with the unit of eV. The values of  $\varepsilon_1(\infty)$ ,  $A_j$ ,  $\Gamma_j$  and  $E_j$  are 3.803, 92.2078, 0.5289 and 4.3172, respectively, taken from Ref. [26].

## 3. RESULTS AND DISCUSSION

Figures 1(a–c) show AFM images and section profiles of nanofeatures formed on silicon by single-shot KrF laser radiation of a regular lattice of PS microspheres ( $2a = 1.0$   $\mu\text{m}$ ) with different laser fluence of 40, 50 and 160  $\text{mJ}/\text{cm}^2$ , respectively. The ablation threshold for PS microspheres is about 33  $\text{mJ}/\text{cm}^2$ .<sup>15</sup> When the PS colloidal monolayer on the Si surface was irradiated with fluences of 40 and 50  $\text{mJ}/\text{cm}^2$ , slightly higher than the ablation threshold of PS microspheres, and ablation occurred on the top surface of the PS spheres, while for this low level laser fluence, the energy density after PS absorption is too low to cause any change on the Si surface. Therefore, upon irradiation with low laser fluence, the previous PS spheres on the Si substrate were partially ablated, and the particles left on the substrate shown in Figures 1(a and b) are PS. The occurrence of the partial ablation of PS spheres at this level fluence can be attributed to their quite strong absorption and low ablation threshold at 248 nm. Moreover, PS nanoflowers were formed upon single pulse

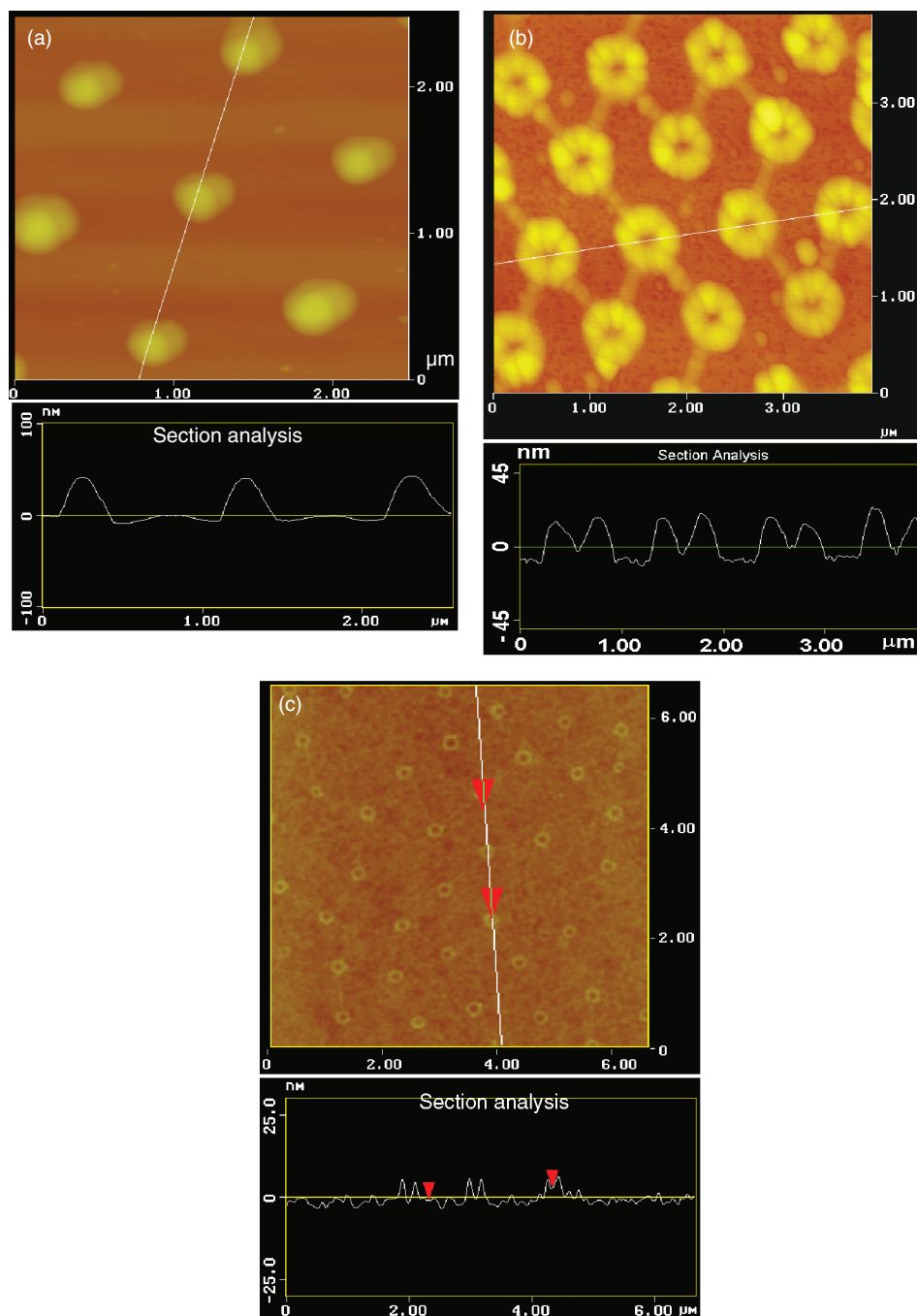


**Fig. 1.** AFM images and section profiles of nanostructures formed on c-Si by single-shot laser radiation with different laser fluence. (a) 40 mJ/cm<sup>2</sup>, (b) 50 mJ/cm<sup>2</sup>, (c) 160 mJ/cm<sup>2</sup>.

irradiation with a laser fluence of 50 mJ/cm<sup>2</sup> shown in Figure 1(b). The formed nanoflower showed a size about 26 nm in height and 600 nm in diameter, as shown in Figures 1(b). The  $z$  position of the centers of nanoflowers is 495 nm. Moreover, the cleaning threshold laser fluence for PS spheres of  $2a = 1 \mu\text{m}$  on Si substrate was about 70 mJ/cm<sup>2</sup>.<sup>15,27</sup> When the laser fluence is much above this cleaning threshold laser fluence, substrate melting and ablation caused by near field focusing became the

predominant cleaning mechanism, leading to the formation of Si nanobumps shown in Figure 1(c). The formed Si nanobumps are with a base diameter about 82 nm and peak height of 7.6 nm.

Figure 2 shows the calculated local amplitude enhancement distribution of the electric field,  $|E|$ , in the  $xy$  planes at different  $z$  positions of  $z_1 = 502 \text{ nm}$  and  $z_2 = 495 \text{ nm}$ . The former is corresponding to the top surface of the bulk c-Si, and the latter represents the position of the centers of

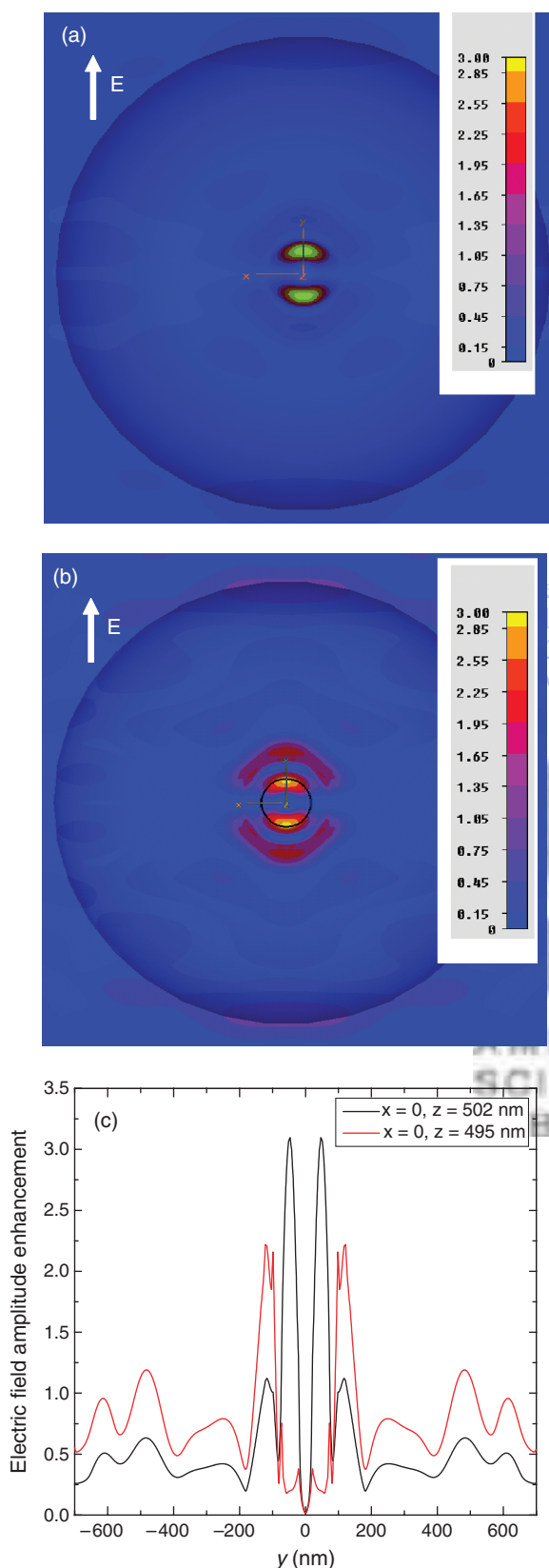


**Fig. 2.** Electric field amplitude  $|E|$  enhancement distribution under PS microsphere in the  $xy$  planes at different  $z$  positions. (a)  $z_1 = 502$  nm, (b)  $z_2 = 495$  nm, (c)  $|E|$  enhancement distributions along the  $y$  axis at  $x = 0$  for (a) and (b).

the formed nanoflowers, i.e., inside PS spheres before the laser irradiation, shown in Figure 1(b). The circumference of the sphere in the  $xy$  planes at various  $z$  positions can be seen clearly from the shadows shown in Figure 2. From the figure, the electric field is enhanced and localized on differently sized domains in both  $xy$  planes. There are two peak spots in the field distribution within the  $x$ - $y$  region. The two small brightest spots in Figure 2 are mainly due to the  $y$  component of the electric field. The peak field enhancement values in the  $xy$  planes at  $z_1 = 502$  nm and  $z_2 = 495$  nm are 3 and 2.3, respectively. This enhancement is smaller than calculated by the Mathematica program based on Mie theory.<sup>15</sup> During the numerical calculation in Ref. [15], only refractive indexes of PS spheres and Si at  $\lambda = 248$  nm was considered. In this work, Drude and Lorentz oscillator models listed in Eqs. (1) and (2) are used for PS spheres and c-Si, respectively. The distance between the centers of both peak spots on the top surface of the bulk c-Si is about 88 nm shown in Figure 2(c). This value is very close to the base diameter of the formed Si nanobump shown in Figure 1(c). The local-field intensity under sphere on the top surface of the bulk c-Si is as large as 3.<sup>27</sup> Because of the near-field enhancement, for the incident laser fluence of  $160$  mJ/cm<sup>2</sup>, the fluence at the contact point between the sphere and the substrate is well above the Si melting threshold at 248 nm of  $500$ – $750$  J/cm<sup>2</sup>.<sup>28</sup> Surface melting of the Si substrate took place within the energy confined area, resulting in the nano-scale modification of the Si surface shown in Figure 1(c). On the other hand, the distance between the centers of the two brightest spots in the  $xy$  plane at the  $z$  position of the centers of formed nanoflowers is larger and about 242 nm. The electric field is mainly enhanced and localized on a domain with a diameter about 400 nm, resulting in formation of nanoflowers with much larger diameter than Si nanobumps.

#### 4. CONCLUSIONS

The combination of theoretical calculations with experimental studies provides an accurate description of near field properties in absorptive spherical polystyrene (PS) micro-particle-Si wafer systems. Near-field flat plane images of PS microspheres were numerically calculated. Nanostructures were prepared on c-Si substrates using the regular 2D arrays by a single pulsed laser irradiation with a wavelength of 248 nm. Periodical PS nanoparticle, PS nanoflowers and Si nanobumps were obtained using different laser fluence. A consistency between the experimental and theoretical results has been achieved.

**Acknowledgments:** This work was supported by National Natural Science Foundation of China (No. 10774046) and Shanghai Municipal Science and Technology Commission Funds (No. 09JC1404600, No. 0852nm06100 and No. 08230705400).

## References and Notes

1. J. Aizenberg, P. V. Braun, and P. Wiltzius, *Phys. Rev. Lett.* **84**, 2997 (2000).
2. Y. Yin, Y. Lu, and Y. Xia, *J. Am. Chem. Soc.* **123**, 771 (2001).
3. C.-M. Hsu, S. T. Connor, M. X. Tang, and Y. Cui, *Appl. Phys. Lett.* **93**, 133109 (2008).
4. K. Lee and S. A. Asher, *J. Am. Chem. Soc.* **122**, 9534 (2000).
5. Y. A. Vlasov, X. Z. Bo, J. C. Sturm, and D. J. Norris, *Nature* **414**, 289 (2001).
6. B. Gates, Y. Yin, and Y. Xia, *Chem. Mater.* **11**, 2827 (1999).
7. I. Schnitzer, E. Yablonovitch, C. Caneau, T. J. Gmitter, and A. Scherer, *Appl. Phys. Lett.* **63**, 2174 (1993).
8. S. M. Huang, Y. Yao, C. Jin, Z. Sun, and Z. J. Dong, *Display* **29**, 254 (2008).
9. M. Stupca, M. Alsalhi, T. Al Saud, A. Almuhanha, and M. H. Nayfeh, *Appl. Phys. Lett.* **91**, 063107 (2007).
10. J. Zhu, Z. Yu, G. F. Burkhard, C.-M. Hsu, S. T. Connor, Y. Xu, Q. Wang, M. McGehee, S. Fan, and Y. Cui, *Nano Lett.* **9**, 279 (2009).
11. S. M. Huang, M. H. Hong, B. S. Luk'yanchuk, Y. W. Zheng, W. D. Song, Y. F. Lu, and T. C. Chong, *J. Appl. Phys.* **92**, 2495 (2002).
12. S. M. Huang, B. S. Luk'yanchuk, M. H. Hong, and T. C. Chong, *Appl. Phys. Lett.* **82**, 4809 (2003).
13. S. M. Huang, M. H. Hong, B. S. Luk'yanchuk, and T. C. Chong, *Appl. Phys. A* **77**, 293, July (2003).
14. S. M. Huang, Z. Sun, B. S. Luk'yanchuk, M. H. Hong, and L. P. Shi, *Appl. Phys. Lett.* **86**, 161911 (2005).
15. S. M. Huang, Z. Sun, and Y. F. Lu, *Nanotechnology* **18**, 025302 (2007).
16. G. Mie, *Ann. Phys.* **25**, 377 (1908).
17. P. A. Bobbert and J. Vlieger, *Physica* **137A**, 209 (1986).
18. Y. Kurokawa, H. Miyazaki, and Y. Jimba, *Phys. Rev. B* **69**, 155117 (2004).
19. L. Landström, N. Arnold, D. Brodoceanu, K. Piglmayer, and D. Bäuerle, *Appl. Phys. A* **83**, 271 (2006).
20. N. Arnold, *Appl. Phys. A* **92**, 1005 (2008).
21. L. Landström, D. Brodoceanu, D. Bäuerle, F. J. Garcia-Vidal, S. G. Rodrigo, and L. Martin-Moreno, *Opt. Exp.* **17**, 761 (2009).
22. A. Pikulin, N. Bityurin, G. Langer, D. Brodoceanu, and D. Bäuerle, *Appl. Phys. Lett.* **91**, 191106 (2007).
23. S. M. Huang, Z. A. Wang, Z. Sun, Z. B. Wang, and B. Luk'yanchuk, *Appl. Phys. A* **96**, 459 (2009).
24. Available at: <http://www.cst.com>.
25. J. G. Carter, T. M. Jelinex, R. N. Hamman, and R. D. Birkhoff, *J. Phys. Chem. Phys.* **44**, 2266 (1966).
26. L. Ding, T. P. Chen, Y. Liu, C. Y. Ng, and S. Fung, *Phys. Rev. B* **72**, 125419 (2005).
27. X. Wu, E. Sacher, and M. Meunier, *J. Appl. Phys.* **87**, 3618 (2000).
28. G. E. Jellison, Jr., D. H. Lowndes, D. N. Mashburn, and R. F. Wood, *Phys. Rev. B* **34**, 2407 (1986).

Received: 30 December 2009. Revised/Accepted: 30 August 2010.

